Optimal design of a high dynamic actuator for diaphragm pumps

S. Vivier, D. Lemoine, G. Friedrich
Université de Technologie de Compiègne (UTC)
Laboratoire d'Electromécanique de Compiègne – EA 1006
60205 COMPIEGNE - FRANCE

***Abstract*- Diaphragm pumps present interests in various applications (artificial hearts, high reliability pumps for nuclear industry…). Nevertheless, they require alternative movements which become difficult to realize for high frequencies with classic movement transformations systems (e.g. cam).**

These types of applications have specific characteristics:

- the mass of the diaphragm is negligible in comparison with the mobile part of the actuator;

- high dynamics linear actuators are required.

Additional constraints are specific to our application:

- low cost;

- high temperature environment.

The paper presents a variable reluctance structure and describes the model and the optimization process used.

A special attention will be paid to the shape optimization authorizing an important gain on the total mass. Finite element simulations will validate the analytical optimization approach and the obtained results.

I. INTRODUCTION

Diaphragm pumps are interesting alternatives to rotary pumps. They are used for various applications such as artificial hearts [1], or high reliability pumps in nuclear industries [2]. Nevertheless, the diaphragm needs to be moved thanks to an alternative actuator. This one is built from a classical rotary motor linked to a movement transformation device, or based on a linear motor.

For high frequencies movements (greater than 200Hz), movement transformations systems become difficult to realize and generate a lack of reliability.

Linear actuators do not have these mechanical problems but require specific studies to design them relatively to specifications.

Another particularity of high dynamic diaphragm pumps is that the moving part of the actuator is much heavier than the diaphragm itself. In a classic linear motor, most of the electric energy injected is used to accelerate and decelerate the moving part of the actuator. To partially avoid this type of problem, the moving part of the actuator needs to be inserted in a resonant mechanical system. In other words, the moving part is linked to one or two springs and operates at a unique frequency supply, roughly equal to the resonance frequency of the mechanical system.

Various electromechanical structures may be used for this application. The most common one is the voice coil structure which is based on the loud speaker principle. The performance of voice coil machines is limited by their specific thrust capability and the flying leads to the current carrying coils. In addition, to limit the mass of the coil, voice coils require high quality magnets and the difficulty of evacuation of copper losses limits the allowed current density and so reduces the specific power of the actuator.

Similar constraints are present for fifteen years in the design of electromagnetic valves. Lot of publications deal with this topic and propose different solutions. In [3], the author describes different structures which associate permanent magnets and variable reluctance configurations. In a more recent publication [4], the author presents, designs and compares various structures of electromagnetic valves. The common point of these applications is that the required force is limited and that the design is mainly imposed by the dynamic constraints.

An interesting structure, developed for a vapor compressor, based on a Hallbach moving part has been described in [5]. Nevertheless, this structure may be difficult to realize and the presence of permanent magnets increases the cost and links the actuator performances to the temperature. The same author describes a frequency tracking system to control this actuator at its resonant frequency [6].

This present paper describes a pure reluctance structure and its optimization. A special attention will be paid to a shape optimization and shows that an optimal design allows an important gain on the actuator mass.

Analytical results are compared to finite element ones, in order to validate the optimal approach.

II. SPECIFICATION BOOK

The specification book is summarized in Table I.

For implantation reasons in the global system, the actuator needs to have a "ring" shape with a minimal internal diameter of 50 mm and a maximum external diameter of 140 mm (see Figure 2).

The actuator should create the more sinusoidal shape movement as possible.

TABLE I
MAIN REQUIRED SPECIFICATIONS

Movement amplitude δ	+/- 4 mm
Frequency f_0	200 Hz
Maximal force *(median position)*	360 N
Diaphragm mass	28 g

III. Device description

The electromechanical structure is presented on Figure 1.

The actuator has an axisymetrical configuration. It is composed of two coils (lower and upper ones), fed separately.

The cross section of the fixed part adopts an E shape, which is symmetrical with the horizontal median plane.

The mobile part is a ring with a trapezoidal cross section. It is free to move linearly and vertically. It is linked to the diaphragm and to one or two springs: these external elements will not be represented in the figures of this article.

The dimensions of the actuator are determined so as to make the magnetic flux cross only one big airgap (e_h) which corresponds to the moving space of the mobile ring. Therefore, the other airgap is reduced to the maximum (e_b), and is used as a mechanical guide for the translation displacement.

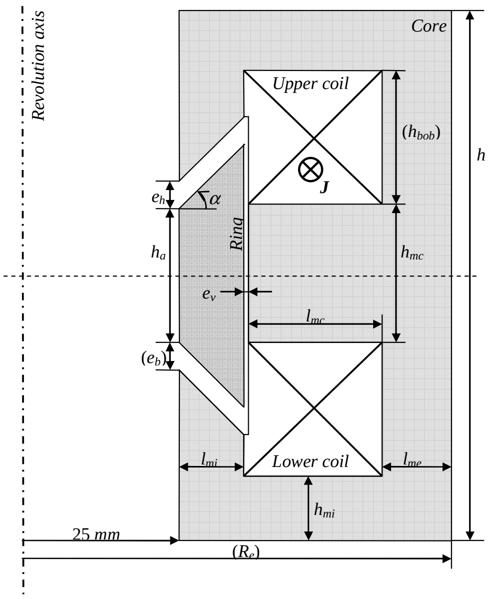

Figure 1: Studied structure

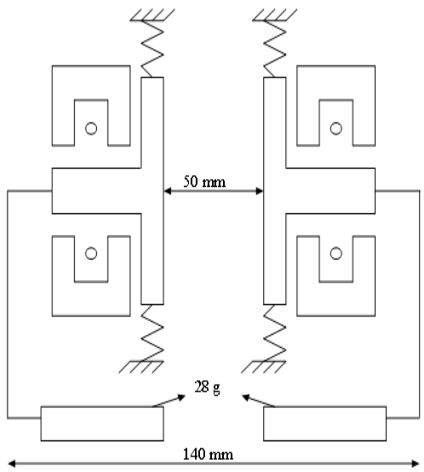

Figure 2: Classic structure

Hence, this geometrical configuration shows a clear advantage with respect to the more classic actuator used with electromagnetic valves [4].

IV. Analytical and Finite element models

A modeling study has been carried out in order to be able to compute the performances (force, movement …) of the actuator, with respect to specific dimensions, and also to initiate an optimization procedure.

In this context, two modeling approaches have been considered. The first one is based on analytical equations, while the second uses the finite element method. In both cases, only the static case is considered. In other words, eddy currents are not computed.

A. *Semi-analytical model*

1) *Electromagnetic model*

The electromagnetic model is fully based on a reluctance network.

The following figure gives an equivalent electrical representation of this network.

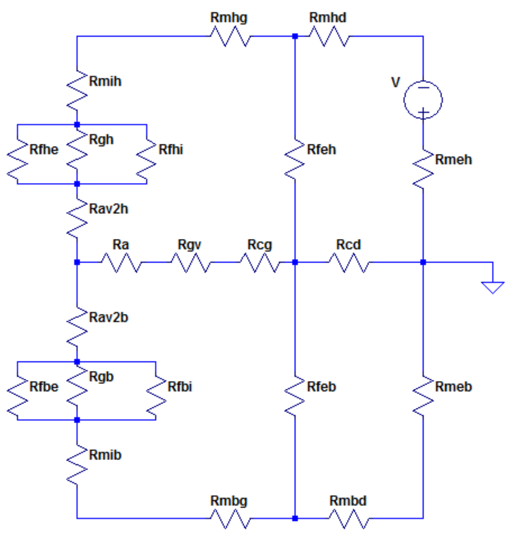

Figure 3: Reluctance network model

This model has been fully implemented under Matlab.

It considers that only the upper coil is fed, and that a current density flows through it (this magnetic source is modeled by the magnetomotive force *V*).

The position of the mobile part is given by the value of the e_h variable, representing the height of the upper displacement airgap. Since the maximum stroke is constant and fixed (8 mm), the height of the lower airgap can be easily deduced.

Reluctances *Rf** model the magnetic losses located in airgaps and yokes. Reluctances *Rm**, *Rc** and *Ra** take account of the magnetic flux flowing in ferromagnetic materials, and therefore of the magnetic saturation phenomenon.

In this context, since these analytical equations depict non linear phenomena, their solving demands the use of numeric methods (such as the Newton-Raphson one) which can only be applied efficiently thanks to computer means.

This situation justifies the use of the “semi-analytical” epithet given to the present model.

The most delicate aspect concerns the calculation of the electromagnetic force F, applied to the mobile part. For this purpose, the following relation has been used:

$$F = \frac{1}{2}.\mathcal{F}^2.\frac{d\boldsymbol{P}}{de_h} \tag{1}$$

Where $\mathcal{F}$ is the magnetomotive force in Figure 4 (that is V in Figure 3) and $\boldsymbol{P}$ the global permeance of the system.

The latter is, of course, dependent on the height of the displacement airgap, that is of the position of the mobile part with respect to the fixed one.

Permeances depending on the airgap heights e_h and e_b, are gathered together (P_{1g} and P_{6g}) in the following figure:

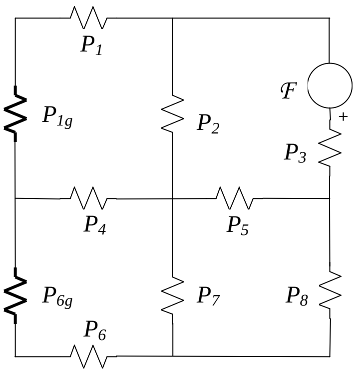

Figure 4: Equivalent permeance network model

The derivative of this global permeance $\boldsymbol{P}$ can be expressed as a combination of partial derivatives, “more easily” written through a formal way:

$$\frac{d\boldsymbol{P}(\boldsymbol{P}_{1g},\boldsymbol{P}_{6g})}{de_h} = \frac{\partial \boldsymbol{P}_{1g}}{\partial e_h}.\frac{\partial \boldsymbol{P}}{\partial \boldsymbol{P}_{1g}} + \frac{\partial \boldsymbol{P}_{6g}}{\partial e_h}.\frac{\partial \boldsymbol{P}}{\partial \boldsymbol{P}_{6g}} \tag{2}$$

In the same time, the analytical model gives naturally access to the computation of related magnetic entities (flux, flux densities, permeabilities …) anywhere in the actuator geometry.

Volumes and masses of the different parts of the actuator are deduced from the volumes and the masses of its different parts.

Finally, subject of hypotheses, some electrical data can be computed as well, such as the number N of turns of each coil, their resistance and inductance ($L=N^2.\boldsymbol{P}$), the current and/or the voltage to apply in order to obtain predefined dynamic behaviors.

2) Dynamic equations

The mobile part is linked to the diaphragm and to springs. The diaphragm is the source of a friction viscous force, while springs exert thrust and return forces. Hence, adding the electromagnetic and the acceleration forces:

$$\frac{d^2x}{dt^2} + \frac{\lambda}{M}.\frac{dx}{dt} + \frac{k}{M}.x = \frac{F_{em}}{M} \tag{3}$$

M is the mass to move. It includes the diaphragm mass, the ring mass as well as a parasite mass related to the spring deformation (which will be neglected).

The previous differential equation corresponds to an oscillatory movement, with a small damping. The diminution of the oscillation amplitudes is caused by the existence of viscous forces ($F_\lambda = -\lambda.dx/dt$) which must be compensated thanks to the electromagnetic force F_{em}.

If this compensation of F_λ *by* F_{em} is exact, the movement behaves like an harmonical oscillator:

$$\frac{d^2x}{dt^2} + \frac{k}{M}.x = 0 \tag{4}$$

Where k is the total stiffness of the springs.

In other words, springs become then the only source of the acceleration force ($F_{acc} = M.d^2x/dt^2$). This is the ideal functioning of the actuator.

If the mobile part is initially shifted by $x(t=0) = \delta/2$ (corresponding to the uppermost position), its position, with respect to time, will be:

$$x(t) = \delta/2.\cos\left(\sqrt{k/M}.t\right) \tag{5}$$

Therefore, the ideal electromagnetic force should satisfy the following temporal expression:

$$F_{em}(t) = \lambda.(\delta/2).\sqrt{k/M}.\sin\left(\sqrt{k/M}.t\right) \tag{6}$$

With the same hypotheses, the median position is reached at $t = T_0/4$, and the corresponding force is maximum:

$$F_0 = \lambda.\delta/2.\sqrt{k/M} = \pi.\lambda.\delta.f_0 \tag{7}$$

The natural frequency f_0 and the stroke δ are given in the specification book.

f_0 is naturally obtained with the appropriate choice of the springs which total stiffness equals $k = M.(2.\pi.f_0)^2$.

Since Table I gives the value of the force to be created, λ can be finally deduced.

3) Power

Instead of considering force values, it may be more interesting to consider the power of the actuator.

The instantaneous power equals:

$$P(t) = F(t).v(t) = F_0.(\delta/2).\omega_0.\sin^2(\omega_0 t) \tag{8}$$

The corresponding average value is:

$$\langle P_m \rangle = \pi.(\delta/2).f_0.F_0 = (\pi^2.\delta^2/2).\lambda.f_0^2 \tag{9}$$

Hence, the force (F_0) being computed thanks to the analytical model, the actuator power can be directly deduced if it is supposed that the stroke of the mobile part ($\delta/2$) and the natural frequency f_0 are known and constant.

To sum up, δ acts on the actuator geometry, λ is linked to the membrane characteristics and f_0 is defined by the choice of the springs.

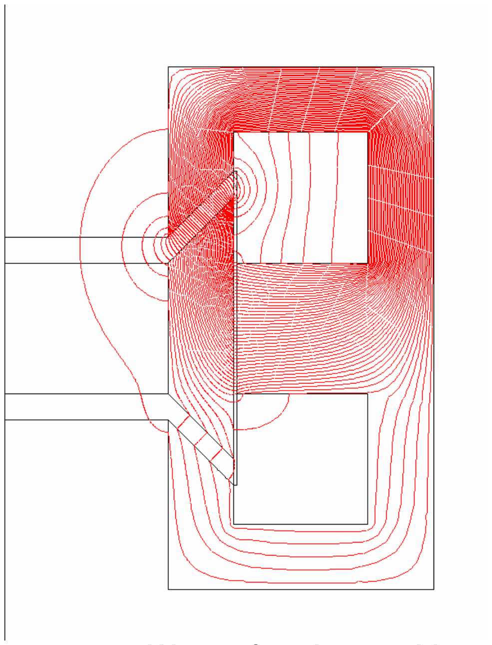

Figure 5: Field lines on finite element model

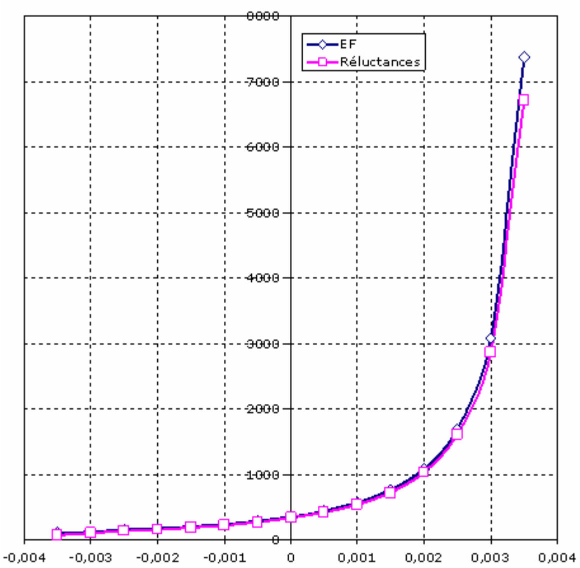

Figure 6: Comparison of analytical and FE models Electromagnetic force (N) versus mobile part position (m)

B. Finite element model

In the same time, the magnetic behavior of the actuator is modeled thanks to a finite element approach. It gives the ability to check the validity of results given by the previous semi-analytical model, for different geometrical and electrical configurations.

Figure 5 gives a view of induction lines when the upper coil is fed with a positive current density.

The study of the main flux paths justify mainly the structure of the reluctance network given in Figure 3a.

It appears clearly that, when the upper coil is fed alone, the mobile part is principally attracted upward (great density of flux lines), but also downward to a lesser degree.

This aspect has been taken into consideration by the analytical modeling.

Figure 6 shows the evolution of the electromagnetic force with respect to the position of the mobile part (from x=-3.5mm to +3.5mm). This force is computed by the two models, for the same geometry and the same electrical supply, with linear magnetic materials here. One observes a good conformity.

The following developments will only consider saturable magnetic materials. The particular cases for which the mobile part touches the fixed armature (i.e. when x=-4 mm and x=+4 mm) have been also considered.

V. Analytical and Finite Element Models

A. Optimization data

1) Input variables

The characteristics that are modified during the optimization process correspond to the dimensions of the actuator. These factors are gathered in Table II.

TABLE II
INPUT VARIABLES (FACTORS)

Name	*Inf. lim.*	*Sup. lim.*	*Unit*	*Description*
h	50	150	mm	*Total height*
l_{mi}	0.5	30	mm	*Width of internal branch*
l_{me}	0.5	30	mm	*Width of external branch*
h_{mi}	0.5	30	mm	*Height of peripheral branches*
l_{mc}	0.5	30	mm	*Width of central branch*
h_{mc}	0.5	30	mm	*Height of central branch*
h_a	0.5	30	mm	*Height of inner side of ring*
α	0	75	deg	*Angle of displacement airgaps*

2) Objective function

One seeks the best combination of factor values that leads to the lightest actuator as possible. The total mass M_{tot} is therefore the objective function of this study.

3) Constraints

Of course, one must consider constraints that define viable actuator geometries.

Moreover, the actuator must be able to create an electromagnetic force, which value can be bounded by two predefined limits. Since the reduction of the actuator dimensions implies naturally a decrease of the generated force, defining these limits is equivalent to impose a minimal force.

So, constraints involve input variables (dimensions of the actuator) as well as output entities (generated force) managed by the analytical model.

B. Optimization algorithm

The optimization method used is called Controlled Weighted Centroïd Method [8]; this is an improved version of the Modified Sequential Simplex Method [7].

It has been implemented under Matlab by the author, using the same calling structure than the traditional optimization functions of the Matlab Optimization Toolbox.

Optimizations take account of predefined tolerances for each input variable, constraint function and output variable. Hence, the algorithm stops as soon as the modification of one of the input variables is lower than a given level, and/or the variation of one of the output variables is higher than a specific reference. This latter characteristic gives the possibility to check the robustness of the optimal solution.

VI. Optimization Process

A. Initial data set

The first data set used in this study has been arbitrarily chosen, but with respect to the lower and upper limits (Table II). This set of eight values is given by Table III.

TABLE III

INITIAL DATA SET

Name	h	l_{mi}	l_{me}	h_{mi}	l_{mc}	h_{mc}	h_a	α
Value	80	10	10	10	20	20	20	45
Unit	mm	mm	mm	mm	mm	mm	mm	deg

The current density is equal to 4 A/mm². The mobile part is fixed to its median position ($e_h=e_b=\delta/2=4$ mm).

Using the previous values leads to an actuator with the following main characteristics:

TABLE IV

ACTUATOR CHARACTERISTICS FROM INITIAL DATA SET

Name	*Value*	*Unit*	*Description*
M_{ring}	0.430	kg	*Mass of the ring*
M_{tot}	7.1	kg	*Total mass of the actuator*
F_{tot}	320	N	*Electromagnetic force*
P_{moy}	904	W	*Average power*
$P_{moy}/M_{tot}\approx 127$ W/kg			

It appears clearly that the actuator is badly proportioned, in view of the important global mass and the too small generated force, with regard to the specification book.

B. Optimization results

The use of the optimization procedure gives the possibility to substantially increase the power/mass ratio.

Approximately one hundred iterations are needed to obtain a first idea of better input variable values. Multiple restarts from previous results with small random additive components are then achieved to ensure the robustness of the optimum characteristics. Finally, the overall optimization process demands five hundred model evaluations at least.

Table V gives the values of the eight input parameters that optimize the actuator relatively to the objective function.

TABLE V

OPTIMIZED CONFIGURATION (J=4 A/mm²)

Name	h	l_{mi}	l_{me}	h_{mi}	l_{mc}	h_{mc}	h_a	α
Value	95.8	8.96	5.17	7.53	13.6	17.3	18.9	54.2
Unit	mm	mm	mm	mm	mm	mm	mm	deg

The corresponding performances are:

TABLE VI

MAIN RESULTS FROM OPTIMIZED CONFIGURATION (J=4 A/mm²)

Name	*Value*	*Unit*	*Description*
M_{ring}	0.396	kg	*Mass of the ring*
M_{tot}	5.17	kg	*Total mass of the actuator*
F_{tot}	362.5	N	*Electromagnetic force*
P_{moy}	911	W	*Average power*
$P_{moy}/M_{tot}=176$ W/kg			

The force is roughly equal to 360 N, as written in the specification book. One notices that the mobile part (ring) is far much heavier than the diaphragm itself, as predicted. This part constitutes hence the main element from a dynamic point of view.

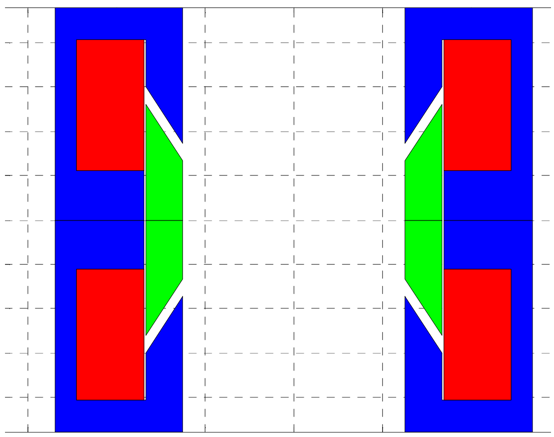

Figure 7: Geometric view of optimized actuator (J=4 A/mm²)

The power/mass ratio increases by almost 38%, mainly because of the strong decrease of the total mass.

A view of the optimized configuration is given by Figure 7.

It appears clearly that no flux density constraints have been imposed in the ferromagnetic parts, since their sections are almost constant and do not depend on the radius.

C. *Extension of the optimization scope*

Results from the previous optimization study have been promising enough to give ideas, to improve again the objective function. In this context, one chooses to increase the current density *J* flowing in the upper coil.

The following tables give the optimized configuration, when *J* is increased to 15 A/mm².

TABLE VII

OPTIMIZED CONFIGURATION (*J*=15 A/mm²)

Name	h	l_{mi}	l_{me}	h_{mi}	l_{mc}	h_{mc}	h_a	α
Value	56.8	6.44	5.09	5.62	8.93	10.4	20.3	48.9
Unit	mm	mm	mm	mm	mm	mm	mm	deg

TABLE VIII

MAIN RESULTS FROM OPTIMIZED CONFIGURATION (*J*=15 A/mm²)

Name	*Value*	*Unit*	*Description*
M_{ring}	0.24	kg	*Mass of the ring*
M_{tot}	2	kg	*Total mass of the actuator*
F_{tot}	360	N	*Electromagnetic force*
P_{moy}	905	W	*Average power*
P_{moy}/M_{tot}*=452 W/kg*			

Figure 8 gives a view of the new configuration. Graduations have same values as in Figure 7.

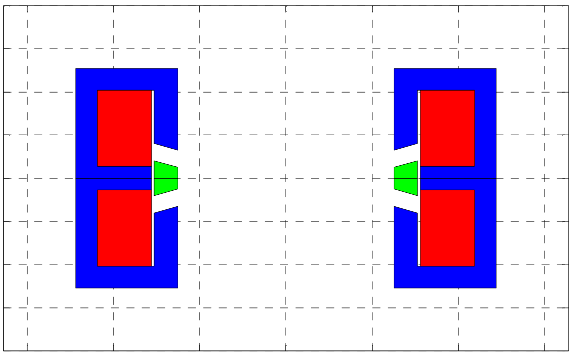

Figure 8: Geometric view of optimized actuator (J=15 A/mm²)

As it could be expected, the modification of the current density is a powerful way to decrease the masses of the different parts of the actuator. However, in the same time:

- magnetic saturation levels increase;

above 20A/mm², the gain on the power/mass ratio becomes negligible;

- thermal constraints are more difficult to satisfy;

the raise of the current density induces an increase of temperatures; even if it is not critical for the current application because of the absence of permanent magnets, this aspect is worth considering.

VII. CONCLUSION

The paper has presented a shape optimization for an oscillating linear actuator.

The paper showed the validity of the proposed electromechanical structure. The gain of actuator mass has demonstrated the interest and the efficiency of the method used.

Nevertheless, some aspects may lead to difficulties:

– the electromagnetic structure and the evolution of the force as a function of the position, may conduct to a difficult control scheme, in order to avoid or limit the shocks between mobile and fixed parts, for extreme positions;

– this study is based on magnetostatic hypotheses; the control of the current and the associated voltage sources to be used in order to reach the required dynamics, remain to be investigated (i.e. as a first step, voltage-imposed sources will have to be substituted for current (density) ones);

– this design is based on a current density approach: a thermal model remains to be developed;

– evaluation of eddy currents should improve the model accuracy.

Other prospective aspects can be imagined. An important one may concern the optimization method, in order to take advantage of the existence of 2 models of the same actuator. In this context, the use of space mapping techniques is certainly promising [9]. Indeed, this type of method exploits low cost demanding models (such as simplified reluctance networks) to approach and in fine to find the optimal conditions precisely given by heavier models (typically finite element models). This approach will certainly improve and speed up the convergence towards the optimum conditions.

REFERENCES

[1] Craven M, Ramphal P, “Design of an electromagnetic pump system for training heart cardiac surgery”, Proceedings IEEE Southeast conf, Kingston, pp. 192-196, 5-7 Apr 2002

[2] Hoffmeister, J. A., “Reliability analysis of pumps for uranium solutions”, IEEE Trans. on Reliability, vol. 37, no. 2, pp. 144-148, Jun 1988

[3] Lequesne B., “Fast acting, long stroke solenoids with two springs”, IEEE Trans. Ind. Appl., vol. 26,no. 5, pp. 848-856, Sep/oct. 1990

[4] Bernez C., “Conception et modélisation d'actionneurs électriques à très forte accélération: application aux soupapes électromagnétiques », PhD Thesis ENS CACHAN, 2006, In french

[5] Wang, Howe, Lin, “Comparative studies on linear motor topologies for reciprocating vapor compressor”, IEMDC07 Conf., CD ROM, 2007

[6] Lin, Wang, Howe, “A resonant frequency tracking for linear vapor compressors”, IEMDC07 Conf., CD ROM, 2007

[7] Routh M.W., Swartz P.A., Denton M.B., “Performance of the Super Modified Simplex”, Analytical Chemistry, Vol.49, N°9, August 1977

[8] Ryan P.B., Barr R.L., Todd H.D., “Simplex Techniques for Nonlinear Optimization”, Analytical Chemistry, Vol.52, pp. 1460-1467, 1980

[9] Tran T.V., Brisset S., Echeverria D., Lahaye D. Brochet P., “Space-mapping techniques applied to the optimization of a safety isolating transformer”, ISEF 2007 Conf., CD ROM, 2007